Dynamics of MODIS evapotranspiration in South Africa

Nebo Jovanovic[1]*, Qiaozhen Mu[2], Richard DH Bugan[1] and Maosheng Zhao[3]

[1]CSIR, Natural Resources and Environment, PO Box 320, 7599 Stellenbosch, South Africa
[2]Numerical Terradynamic Simulation Group, College of Forestry and Conservation, University of Montana, 32 Campus Drive, Missoula, MT 59812, USA
[3]Department of Geographical Sciences, University of Maryland, 2181 Samuel J. LeFrak Hall, College Park, MD 20742, USA

ABSTRACT

This paper describes the dynamics of evapotranspiration (*ET*) in South Africa using MOD16 ET satellite-derived data, and analyses the inter-dependency of variables used in the *ET* algorithm of Mu et al. (2011). Annual evapotranspiration is strongly dependent on rainfall and potential evapotranspiration (*PET*) in 4 climatically different regions of South Africa. Average *ET* in South Africa (2000–2012) was estimated to be 303 mm·a^{-1} or 481.4 x 10^9 m^3·a^1 (14% of *PET* and 67% of rainfall), mainly in the form of plant transpiration (*T*, 53%) and soil evaporation (*Soil E*, 39%). Evapotranspiration *(ET)* showed a slight tendency to decrease over the period 2000–2012 in all climatic regions, except in the south of the country (winter rainfall areas), although annual variations in *ET* resulted in the 13-year trends not being statistically significant. Evapotranspiration *(ET)* was spatially dependent on *PET*, *T* and vapour pressure deficit *(VPD)*, in particular in winter rainfall and arid to semi-arid climatic regions. Assuming an average rainfall of 450 mm·a^{-1}, and considering current best estimates of runoff (9% of rainfall), groundwater recharge (5%) and water withdrawal (2%), MOD16 ET estimates were about 15% short of the water balance closure in South Africa. The *ET* algorithm can be refined and tested for applications in restricted areas that are spatially heterogeneous and by accounting for soil water supply limiting conditions.

Keywords: MOD16, potential evapotranspiration, soil evaporation, transpiration, water balance

INTRODUCTION

Sustainable management of water resources requires careful planning, monitoring and management, as water is a finite resource in quality and quantity. Environmental change driven by anthropogenic global warming imposes additional constraints, for example, increase in extreme weather occurrences (droughts and floods), increase in temperature and potential evaporation, changes in rainfall amounts and distribution, etc. The quantification of the water cycle components is a fundamental requirement in the assessment and management of water resources, in particular, under the impacts of human-induced land-use and climate change.

Evapotranspiration (*ET*) is a key process within the hydrological cycle and arguably the most difficult component to determine, especially in arid and semi-arid areas where a large proportion of low and sporadic precipitation is returned to the atmosphere via *ET*. In these areas, vegetation is often subject to water stress and plant species adapt in different ways to prolonged drought conditions (Jovanovic and Israel, 2012). Evapotranspiration *(ET)* is estimated to be >60% of rainfall on a global scale (Korzoun et al., 1978; L'vovich and White, 1990) and can reach nearly 100% of rainfall in arid regions (Bugan et al., 2012). In addition, *ET* varies depending on the heterogeneity of the landscape and topography, climate, type of vegetation and soil properties (Mu et al., 2007a). This makes the process of *ET* very dynamic over time and variable in space. By understanding how this parameter varies in space and time, we will improve our understanding of a critical component of the water cycle.

Besides the FLUXNET network (Baldocchi et al., 2001), measurements of *ET* are scarce and localised. However, our ability to use information from satellite sensors to estimate *ET* is developing rapidly and offers the opportunity to understand how *ET* varies across space and time, reduce uncertainty levels, increase spatial details and scale-up to large areas. The accuracy and uncertainty of satellite-based estimates of *ET* were evaluated in specific studies for different algorithms and products, e.g., SEBAL (Bastiaanssen et al., 1998a and b), METRIC (Allen et al., 2007a and b), SEBS (Su, 2002), and MODIS ET (Mu et al., 2007a), as well as for components of *ET* calculation such as MODIS fraction of absorbed photosynthetically active radiation (*FPAR*) and leaf area index (*LAI*) (Myneni et al., 2002). This was generally done by comparison between remote sensing–based estimates of *ET* and ground-based measurements of *ET* or other variables. Mueller et al. (2011) and Jimenez et al. (2011) also compared global *ET* datasets and surface fluxes obtained with satellite-based products and land surface models for large river basins of the world.

The Council for Scientific and Industrial Research (CSIR) has recently initiated research aimed at evaluating, validating and improving the MOD16 ET product, one of the free satellite-based *ET* products with readily available *ET* data for the past 13 years. These time series were seldom applied to estimate *ET* in Africa, especially in arid and semi-arid regions. The MOD16 ET product estimates global *ET* from ground-based meteorological observations and remote-sensing data from the Moderate Resolution Imaging Spectroradiometer (MODIS) located on NASA's Terra and Aqua satellites (Justice et al., 2002). The MODIS sensor works on a spatial resolution of approximately 1 km, making it potentially suitable for applications in water resource management. The images contain 36 spectral bands in the wavelength range of 0.4 to 14.4 μm. The MOD16 ET algorithm was developed by Mu et al. (2007a) from the original model of Cleugh et al. (2007), and later improved by Mu et al.

---

*   To whom all correspondence should be addressed.
☎ 27 21 888 2506; Fax: +27 21 888 2682;
    e-mail: njovanovic@csir.co.za

(2011). This paper presents the first evaluation of the MOD16 ET done in South Africa at country-wide scale. The aims were: (i) to describe the annual and spatial trends of *ET* and its components estimated with the modified *ET* algorithm of Mu et al. (2011) for South Africa, and (ii) to assess the limiting ranges of algorithm key variables in relation to *ET* and its components.

MATERIAL AND METHODS

MOD16 ET algorithm

Brief description of the MOD16 ET algorithm

The detailed algorithm description can be found in Mu et al. (2007a) and Mu et al. (2011). In this study, only the variables used in the analysis are described. The MOD16 ET algorithm is based on the physically sound theory of the Penman-Monteith energy balance (Monteith, 1965; Allen et al., 1998):

$$\lambda ET = \frac{\Delta(R_n - G) + \rho C_p (e_s - e_a)/r_a}{\Delta + \gamma \times (1 + r_s/r_a)} \qquad (1)$$

where:

ET is in mm
λ is the latent heat of vaporisation of water (J·kg^{-1})
Δ is the gradient of the saturation vapour pressure-temperature function (Pa·°C^{-1})
R_n is the net radiation (J·m^{-2}·s^{-1})
G is the soil heat flux (J·m^{-2}·s^{-1})
ρ_a is the air density (kg·m^{-3})
C_p is the specific heat of the air (J·kg^{-1}·K^{-1})
e_s is the saturated vapour pressure of the air (Pa), a function of air temperature measured at height *z*
e_a is the mean actual vapour pressure of the air measured at height *z* (Pa)
$(e_s - e_a)$ is vapour pressure deficit (*VPD*; Pa)
r_a is the aerodynamic resistance to water vapour diffusion into the atmospheric boundary layer (s·m^{-1})
γ is the psychrometric constant (0.066 kPa·K^{-1})
r_s is the surface resistance to water vapour transfer (s·m^{-1})

The MOD16 ET algorithm (Mu et al., 2011) calculates *ET* using global daily temperature, actual vapour pressure and incoming solar radiation, and remotely-sensed *LAI*, *FPAR*, albedo, and land cover type. The available energy at the land surface (R_n) is partitioned into vegetation surface and soil surface using *FPAR* (MODIS 15A product, assumed to be equal to canopy cover F_C). The term r_s from Eq. (1) is defined as an effective surface resistance to evaporation from the soil surface and transpiration from the plant canopy. Canopy r_s decreases as *VPD* decreases, and it is also limited by low temperature (Mu et al., 2007a; Mu et al., 2011).

Evaporation from the wet canopy occurs after certain conditions (e.g. after rainfall, when air relative humidity >70%) and can be a substantial component when leaf area is large. In order to calculate daytime and night-time *ET*, daily average air temperature (*Tavg*) is assumed to be the average of daytime air temperature (*Tday*) and night-time temperature (Mu et al., 2011). Day-time and night-time *ET* are then added up to get daily *ET* values.

A soil evaporation (*Soil E*) component is also calculated in the MOD16 ET algorithm (Mu et al., 2011), which may be important in areas with a sparse canopy. The potential evaporation from the soil is first calculated with an equation that fully resembles the Penman-Monteith energy balance equation (Eq. (1)). Actual *Soil E* is then calculated as a function of air relative humidity (*RH*). The algorithm also considers the wet surface fraction (F_{wet}) calculated as a function of *RH*. The wet surface fraction (F_{wet}) represents the fraction of canopy or soil covered by water. In the case of the canopy, F_{wet} is used to separate evaporation of water intercepted by the canopy and transpiration (*T*). In the case of the soil, F_{wet} is used to separate evaporation from saturated and moist soil surface. The latent heat fluxes from vegetation canopy and soil (partitioned through F_C and F_{wet}) are finally summed up to calculate *ET* for the particular vegetation.

MOD16 ET is the sum of 3 components:

$$ET = T_c + E_s + E_i \qquad (2)$$

where:

T_c, E_s, and E_i are canopy transpiration (*T*), soil evaporation (*Soil E*), and interception evaporation (*Canopy E*), respectively.

$$\lambda T_c = \frac{(\Delta R_n F_C + \rho C_p VPD\, F_C/r_{ac})(1 - Fwet)}{s + \gamma \times (1 + r_{sc}/r_{ac})} \qquad (3)$$

$$\lambda E_i = \frac{(\Delta R_n F_C + \rho C_p VPD\, F_C/r_{awc})Fwet}{\Delta + \left(1 + {r_{swc}}/{r_{awc}}\right)} \qquad (4)$$

The term E_s consists of *Soil E* from dry soil surface and wet soil surface:

$$E_s = E_{wet\_soil} + E_{SoiLpot}\, f_{sm} \qquad (5)$$

$$\lambda E_{wet\_SOIL} = \frac{\left(\Delta(R_n(1 - F_c) - G) + \rho C_p(1.0 - F_C)\, VPD/r_{as}\right)Fwet}{s + \left(1 + {r_{ss}}/{r_{as}}\right)} \qquad (6)$$

$$\lambda E_{SOILpot} = \frac{\left(\Delta(R_n(1 - F_c) - G) + \rho C_p(1.0 - F_C)\, VPD/r_{as}\right)(1 - Fwet)}{s + \left(1 + {r_{ss}}/{r_{as}}\right)} \qquad (7)$$

where:

F_C is the fractional vegetation cover
F_{wet} is relative surface wetness (RH^4)
r_{ac}, r_{sc} are the aerodynamic and canopy resistances of the dry canopy
f_{sm} is modified RH^{VPD} to the one in Fisher et al. (2008)
r_{awc} and r_{swc} are the aerodynamic and wet canopy resistances of the wet canopy
ET_{wet_soil} and $ET_{SOILpot}$ are the wet and potential *Soil E*
r_{as} and r_{ss} are the soil aerodynamic conductance and soil total resistances

The potential plant transpiration (T_{pot}) is calculated following the Priestley-Taylor (Priestley and Taylor, 1972) equation:

$$\lambda T_{pot} = \frac{\alpha \Delta R_n F_C(1 - Fwet)}{s + \gamma}, \alpha = 1.26 \qquad (8)$$

The total daily potential *ET (PET)* is calculated with Eq. (9):

$$PET = \lambda E_i + \lambda T_{pot} + \lambda E_{wet\_SOIL} + \lambda E_{SOILpot} \qquad (9)$$
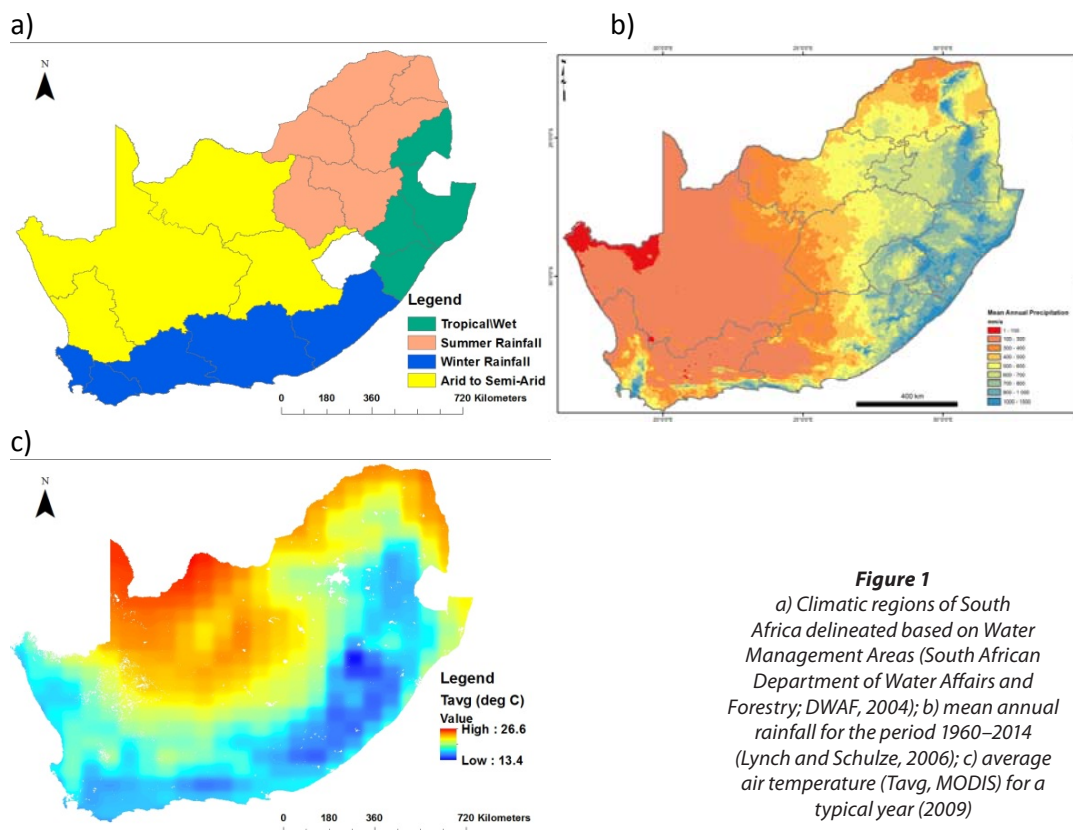
Figure 1
a) Climatic regions of South Africa delineated based on Water Management Areas (South African Department of Water Affairs and Forestry; DWAF, 2004); b) mean annual rainfall for the period 1960–2014 (Lynch and Schulze, 2006); c) average air temperature (Tavg, MODIS) for a typical year (2009)

GMAO MERRA meteorological input data

NASA/GMAO Modern Era Retrospective Analysis (MERRA) at spatial resolution of 0.5˚x 0.66˚ provided every hour was used as meteorological input to the MOD16 ET algorithm. Mu et al. (2011) processed the hourly data to daily level. The technique proposed by Zhao et al. (2005) was used to interpolate data from coarse spatial resolution to 1 km, to fit MODIS pixels, to remove abrupt changes from one side of a GMAO pixel to another, and to improve the accuracy of these pixels.

Methodology and study area

South Africa covers a wide range of climatic and hydrological conditions. The South African Department of Water Affairs classified the country's water resources into 19 water management areas (WMAs) in 2004 (DWAF, 2004, since regrouped into 9 WMAs). The WMA borders were used to delineate 4 climatic regions (Fig. 1a). The western and central WMAs fall in arid and semi-arid regions. The southern WMAs are in an area with a Mediterranean (winter rainfall) climate. The eastern coastal area has a tropical wet climate, whilst the northern regions are in the sub-tropical (summer rainfall) belt. Such climatic diversity is ideal for the analysis of a wide range of *ET* values. The division into 4 climatic regions is corroborated by the characteristic gradient in annual rainfall from west (arid and semi-arid climate) to east (tropical wet climate) (Fig. 1b; Lynch and Schulze, 2006). It is evident that average air temperatures are typically moderate in the south and east of the country, and high in the north-west (Fig. 1c).

Thirteen years (2000–2012) of annual MOD16 ET and GMAO MERRA meteorological data were collected and processed for the whole country, as well as for individual climatic

regions as classified in Fig. 1a, on a 0.912 km x 0.912 km pixel basis. For each yearly data set, the following variables were extracted:

- Evapotranspiration (*ET*)
- Potential evapotranspiration (*PET*)
- Evaporation from wet canopy surface (*Canopy E*)
- Soil evaporation (*Soil E*)
- Dry soil evaporation (*Dry soil E*)
- Wet soil evaporation (*Wet soil E*)
- Transpiration (*T*)
- Average air temperature (*Tavg*)
- Daytime average air temperature (*Tday*)
- Daytime average vapour pressure deficit (*VPD*)

The variables were selected based on the improvements introduced by Mu et al. (2011) to the original algorithm. Yearly and spatial changes in *ET* were analysed and correlated to the yearly values for each variable in order to assess the sensitivity and dependence of *ET* to the selected variables. The data were analysed for the whole country as well as per climatic region.

Statistical analysis

The temporal (annual) changes in *ET* and associated variables were assessed using linear regression functions and tested for statistical significance. For the assessment of dependence between *ET* and associated variables over time, the Spearman rank correlation coefficient (r_s) was used because it is suitable for small data series that may not necessarily have a normal distribution. The InfoStat software (Di Rienzo et al., 2012) was used for the calculation of r_s and statistical significance.

For the spatial analysis it was not possible to generate a dataset by averaging the annual data for 13 years because the

TABLE 1
**Potential evapotranspiration (*PET*), actual evapotranspiration (*ET*), canopy and soil evaporation
(*Canopy E* and *Soil E*) and transpiration (*T*) estimated with MODIS products for South Africa.
Slopes of the linear regression are shown (*p*>0.05 in all cases). Total area is 1 228 297 km².**

| Year	*PET* (mm·a⁻¹)	*ET* (billion m³·a⁻¹)	*ET* (mm·a⁻¹)	*Canopy E* (mm·a⁻¹)	*Soil E* (mm·a⁻¹)	*T* (mm·a⁻¹)	*ET/ PET*	*Canopy E/ET*	*Soil E/ET*	*T/ET*
2000	2 173	428.1	349	41	139	169	0.16	0.12	0.40	0.48
2001	2 174	411.9	335	30	138	167	0.15	0.09	0.41	0.50
2002	2 292	340.3	277	18	103	156	0.12	0.07	0.37	0.56
2003	2 321	299.2	244	14	93	137	0.10	0.06	0.38	0.56
2004	2 285	342.2	279	21	95	163	0.12	0.07	0.34	0.58
2005	2 266	340.4	277	24	107	146	0.12	0.09	0.39	0.53
2006	2 156	434.3	354	42	142	169	0.16	0.12	0.40	0.48
2007	2 268	347.1	283	22	110	151	0.12	0.08	0.39	0.53
2008	2 211	377.4	307	27	129	151	0.14	0.09	0.42	0.49
2009	2 236	377.6	307	30	122	156	0.14	0.10	0.40	0.51
2010	2 262	369.8	301	27	116	159	0.13	0.09	0.38	0.53
2011	2 209	393.5	320	26	119	175	0.15	0.08	0.37	0.55
2012	2 250	368.8	300	24	115	162	0.13	0.08	0.38	0.54
Average	2 239	371.6	303	27	117	158	0.14	0.087	0.387	0.526
Slope	0.649	−0.097	−0.079	−0.153	−0.203	0.277	−1E-04	−2E-04	−3E-04	5E-04

number of missing data (out of range) varied between years, and this may have introduced inconsistencies and bias. The spatial analysis was then performed for a year when annual *ET* and associated components exhibited the least deviation from the 13-year average. This typical year was 2009 and it was assumed that it would give a realistic and representative description of spatial differences. Average, median, standard deviation, coefficient of variation, skewness and kurtosis of all relevant variables were determined using all data pixels. The spatial dependence between variables was assessed for all years using the coefficient of determination (R^2) of regression functions and Pearson correlation coefficient (r). In this instance, r was used instead of r_s to reduce computation time because of the very large dataset (n>100 000) and to better account for outliers (the effects of outliers may be masked by the ranking in r_s). Both the coefficient of determination (R^2) and the correlation coefficients were reported to be suitable to indicate whether two datasets have similar temporal or spatial patterns (Ji and Gallo, 2006).

RESULTS AND DISCUSSION

Temporal changes of MOD16 ET and *ET* components

Thirteen years of annual *PET*, *ET* and its components were estimated with MODIS products and are shown in Table 1. It was estimated that the average *ET* in South Africa is 303 mm·a⁻¹, ranging from 244 mm·a⁻¹ in 2003 to 354 mm·a⁻¹ in 2006. Only 14% of the potential atmospheric demand for water evaporates (*ET/PET*). The largest component of *ET* was transpiration of plants (53% on average), followed by *Soil E* (39% on average). Direct evaporation from the vegetation canopy was a minor component of *ET* (9% on average).

Annual values indicated that *ET* was rather stable in the period 2000–2012 (Fig. 2), depending on rainfall amounts and distribution. Evapotranspiration (*ET*), *Canopy E* and *Soil E* showed a slight tendency to decrease based on the negative slope of the linear regression (Table 1), whilst *PET* and *T* were slightly increasing (positive slope in Table 1). However, annual variability was much larger than the observed changes and
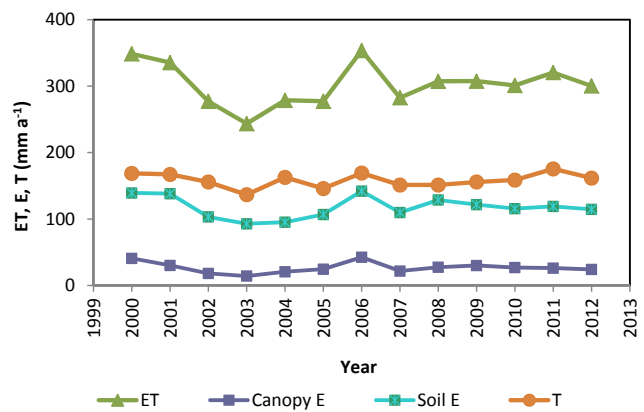
Figure 2
Thirteen-year trends in annual evapotranspiration (ET), canopy evaporation (canopy E), soil evaporation (soil E) and transpiration (T) estimated with MODIS for South Africa

these trends were not statistically significant (*p*>0.05). Tables 2 to 5 show 13 years of annual *PET*, *ET* and its components for each climatic region. Evapotranspiration (*ET*) displayed a slight tendency to decrease in all climatic regions, except in winter rainfall areas where the *Canopy E* and *Soil E* were increasing. However, none of the trends was statistically significant (*p*>0.05). Nation-wide average values (Table 1) are biased towards the values estimated in the arid and semi-arid climate, which represents the largest climatic region in extent (Fig. 1a).

The relations between variables were determined using r_s and the results are summarised in Table 6. The values below the main diagonal in Table 6 represent r_s. A positive number represents positive correlation and vice versa. Good correlations tend to +1 (positive correlation) and −1 (negative correlation). The values above the main diagonal represent the probability associated with the null hypothesis. Values <0.05 represent statistically significant relations at probability of 95% or more, and these are highlighted in bold in Table 6. It is evident that there is generally a negative correlation between *PET* and all

TABLE 2
**Potential evapotranspiration (*PET*), actual evapotranspiration (*ET*), canopy and soil evaporation (*Canopy E*
and *Soil E*) and transpiration (*T*) estimated with MODIS products for the summer rainfall area of South Africa.
Slopes of the linear regression are shown (*p*>0.05 in all cases). Total area is 299 693 km².**

Year	PET (mm·a⁻¹)	ET (billion m³·a⁻¹)	ET (mm·a⁻¹)	Canopy E (mm·a⁻¹)	Soil E (mm·a⁻¹)	T (mm·a⁻¹)	ET/ PET	Canopy E/ET	Soil E/ET	T/ET
2000	2157	105.9	460	46	161	254	0.21	0.1	0.35	0.55
2001	2200	93.1	405	27	139	239	0.18	0.07	0.34	0.59
2002	2370	66.7	290	8	83	198	0.12	0.03	0.29	0.68
2003	2396	59.5	259	6	72	181	0.11	0.02	0.28	0.7
2004	2263	80.6	350	17	93	241	0.15	0.05	0.26	0.69
2005	2312	72.5	315	15	97	203	0.14	0.05	0.31	0.64
2006	2147	103.1	448	53	162	233	0.21	0.12	0.36	0.52
2007	2329	73.5	320	12	95	213	0.14	0.04	0.3	0.67
2008	2244	86.7	377	28	135	213	0.17	0.08	0.36	0.57
2009	2231	94.1	409	40	141	229	0.18	0.1	0.34	0.56
2010	2260	89.5	389	26	117	246	0.17	0.07	0.3	0.63
2011	2303	84.6	368	20	105	243	0.16	0.05	0.29	0.66
2012	2329	76.3	332	13	95	224	0.14	0.04	0.29	0.68
Average	2272	83.5	363	24	115	224	0.16	0.06	0.31	0.63
Slope	3.278	−0.068	−0.296	−0.256	−0.746	0.705	−5E-04	−5E-05	−1E-03	−2E-03

TABLE 3
**Potential evapotranspiration (*PET*), actual evapotranspiration (*ET*), canopy and soil evaporation (*Canopy E*
and *Soil E*) and transpiration (*T*) estimated with MODIS products for the tropical wet area of South Africa.
Slopes of the linear regression are shown (*p*>0.05 in all cases). Total area is 132 913 km².**

Year	PET (mm·a⁻¹)	ET (billion m³·a⁻¹)	ET (mm·a⁻¹)	Canopy E (mm·a⁻¹)	Soil E (mm·a⁻¹)	T (mm·a⁻¹)	ET/ PET	Canopy E/ET	Soil E/ET	T/ET
2000	1 834	108.4	816	192	249	375	0.44	0.24	0.31	0.46
2001	1 869	101.5	764	148	220	395	0.41	0.19	0.29	0.52
2002	1 935	90.6	682	98	180	404	0.35	0.14	0.26	0.59
2003	1 970	80.9	609	77	181	351	0.31	0.13	0.3	0.58
2004	1 906	92.5	696	107	179	410	0.37	0.15	0.26	0.59
2005	1 905	92.2	694	130	212	352	0.36	0.19	0.31	0.51
2006	1 823	104.5	787	178	234	375	0.43	0.23	0.3	0.48
2007	1 935	92.2	694	108	200	385	0.36	0.16	0.29	0.56
2008	1 853	91.9	691	126	234	331	0.37	0.18	0.34	0.48
2009	1 880	96.2	724	140	211	373	0.39	0.19	0.29	0.52
2010	1 922	94.8	713	136	216	362	0.37	0.19	0.3	0.51
2011	1 857	94.2	709	119	201	389	0.38	0.17	0.28	0.55
2012	1 910	94.8	713	118	199	396	0.37	0.17	0.28	0.56
Average	1 892	95.0	715	129	209	377	0.38	0.18	0.29	0.53
Slope	0.002	−0.313	−2.356	−1.292	−0.368	−0.696	−1E-0.3	−6E-04	2E-04	4E-04

variables except *T/ET*. The remaining variables were generally positively correlated. Analysis by climatic region indicated that the correlations of ratios (*Canopy E/ET*, *Soil E/T* and *T/ET*) to other variables were generally not significant in the winter rainfall and especially arid and semi-arid climates.

In absolute terms, MOD16 ET estimated an average water loss to the atmosphere of 371.6 x 10⁹ mm·a⁻¹ for the country (Table 1). Assuming an average rainfall of 450 mm·a⁻¹, corresponding to 553 x 10⁹ mm·a⁻¹, it was calculated that 67% of rainfall water evaporates. It was estimated that runoff is about 50 x 10⁹ mm·a⁻¹ or 9% of rainfall (DWAF, 2004) and that groundwater recharge is about 30 x 10⁹ mm·a⁻¹ or 5% of rainfall (Vegter, 1995; DWAF, 2005). Frenken (2005) estimated water withdrawal in South Africa to be 12.5 x 10⁹ mm·a⁻¹ in 2000. Considering missing data (about 3% of the total number of pixels), MOD16 ET estimates were about 15% short of the water balance closure for South Africa, possibly due to inaccuracies in the algorithm and input data (e.g. land cover).

Spatial changes of MOD16 ET and *ET* components

Figure 3 (a to g) displays environmental variables obtained from MODIS for a typical year (2009) when annual *ET* and associated components exhibited the least deviations from the 13-year average (Table 1). Climatic conditions drive *PET* exhibiting a gradient from the southeast to the northwest (Fig. 3a). The gradient is inverse for *ET* (Fig. 3b), which is driven by atmospheric evaporative demand, but depends on rainfall (Fig. 1b) and vegetation cover (Fig. 3c). High rainfall areas (Fig. 1b) are generally associated with a more humid

TABLE 4
Potential evapotranspiration (*PET*), actual evapotranspiration (*ET*), canopy and soil evaporation (*Canopy E* and *Soil E*) and transpiration (*T*) estimated with MODIS products for the winter rainfall area of South Africa. Slopes of the linear regression are shown (*p*>0.05 in all cases). Total area is 249 637 km².

Year	*PET* (mm·a⁻¹)	*ET* (billion m³·a⁻¹)	*ET* (mm·a⁻¹)	*Canopy E* (mm·a⁻¹)	*Soil E* (mm·a⁻¹)	*T* (mm·a⁻¹)	*ET/ PET*	*Canopy E/ET*	*Soil E/ET*	*T/ET*
2000	1 886	103.4	414	43	191	180	0.22	0.1	0.46	0.43
2001	1 899	102.7	411	36	189	186	0.22	0.09	0.46	0.45
2002	1 965	94.2	377	27	162	189	0.19	0.07	0.43	0.5
2003	1 963	87.5	351	21	156	173	0.18	0.06	0.45	0.49
2004	2 001	90.1	361	25	156	180	0.18	0.07	0.43	0.5
2005	1 940	95.0	380	33	170	177	0.20	0.09	0.45	0.46
2006	1 856	109.0	436	49	203	184	0.24	0.11	0.47	0.42
2007	1 933	97.2	389	34	181	175	0.20	0.09	0.46	0.45
2008	1 898	99.2	397	34	187	176	0.21	0.09	0.47	0.44
2009	1 957	89.6	359	27	172	160	0.18	0.07	0.48	0.45
2010	1 960	91.6	367	29	185	154	0.19	0.08	0.5	0.42
2011	1 836	106.5	426	40	194	193	0.23	0.09	0.45	0.45
2012	1 869	106.6	427	40	193	194	0.23	0.09	0.45	0.46
Average	1 920	97.9	392	34	180	179	0.20	0.08	0.46	0.46
Slope	−3.719	0.297	1.188	0.235	1.323	−0.369	1E-03	3E-04	2E-03	−2E-03

TABLE 5
Potential evapotranspiration (*PET*), actual evapotranspiration (*ET*), canopy and soil evaporation (*Canopy E* and *Soil E*) and transpiration (*T*) estimated with MODIS products for the arid and semi-arid area of South Africa. Slopes of the linear regression are shown (*p*>0.05 in all cases). Total area is 546 054 km².

Year	*PET* (mm·a⁻¹)	*ET* (billion m³·a⁻¹)	*ET* (mm·a⁻¹)	*Canopy E* (mm·a⁻¹)	*Soil E* (mm·a⁻¹)	*T* (mm·a⁻¹)	*ET/ PET*	*Canopy E/ET*	*Soil E/ET*	*T/ET*
2000	2 400	80.3	147	1	77	70	0.06	0.01	0.52	0.47
2001	2 365	87.6	160	1	93	66	0.07	0	0.58	0.41
2002	2 494	68.4	125	0	67	58	0.05	0	0.53	0.47
2003	2 537	53.0	97	0	52	45	0.04	0	0.54	0.46
2004	2 524	55.7	102	0	47	55	0.04	0	0.47	0.54
2005	2 485	59.2	108	0	56	52	0.04	0	0.52	0.48
2006	2 384	87.9	161	2	80	79	0.07	0.01	0.5	0.49
2007	2 477	62.2	114	0	62	52	0.05	0	0.54	0.46
2008	2 430	74.2	136	0	72	64	0.06	0	0.53	0.47
2009	2 458	71.0	130	0	66	63	0.05	0	0.51	0.49
2010	2 490	68.3	125	0	58	67	0.05	0	0.46	0.54
2011	2 424	83.0	152	1	70	81	0.06	0	0.46	0.53
2012	2 473	68.0	125	0	67	57	0.05	0	0.54	0.46
Average	2 457	70.7	129	0	67	62	0.05	0.00	0.52	0.48
Slope	1.528	−0.018	−0.032	−0.014	−0.614	0.596	−8E-05	−3E-04	−4E-03	4E-03

environment, lower *PET* and denser vegetation cover compared to dry areas. As a result, *ET* is higher in the tropical wet eastern region compared to the arid and semi-arid northwest region (Fig. 3b). Both components of *ET*, namely *T* (Fig. 3d) and *Soil E* (Fig. 3e), exhibit the same gradients, i.e., they are high in the high rainfall area of the east coast and low in the arid northwest of the country.

The MODIS land cover map (Fig. 3c) classifies the largest portion of inland South Africa (central and western regions) as open shrubland and grassland, with savanna occurring in the northeast part of the country. Land cover is classified as cropland mostly along the west and east coast and in the northeast. The main urban areas are clearly visible in the northeast (Johannesburg), southwest (Cape Town) and on the east coast (Durban). Values of MODIS variables were out of range for pixels coinciding with urban areas and these were discarded from the analysis. Another area with frequent missing data (out of range) is visible in the northwest inland and classified as barren or sparsely vegetated. The ratio *T/ET* tends to be high in the northern, summer rainfall parts of the country where grasslands commonly occur, and low in the dry southwest where sparse vegetation occurs (Fig. 3f). The opposite trend is visible for the *Soil E/ET* ratio (Fig. 3g). In the central and northwestern parts of the country, lines following major river systems (Orange and Vaal) are clearly visible providing exceptional values of high *T/ET* and low *Soil E/ET* (Figs 3f and g).

Table 7 shows the statistical analysis of MODIS spatial data for a typical year (2009). For *ET* and related variables (*Soil E* and *T*), the large standard deviations and coefficients of variation indicated the wide ranges of values observed. The median
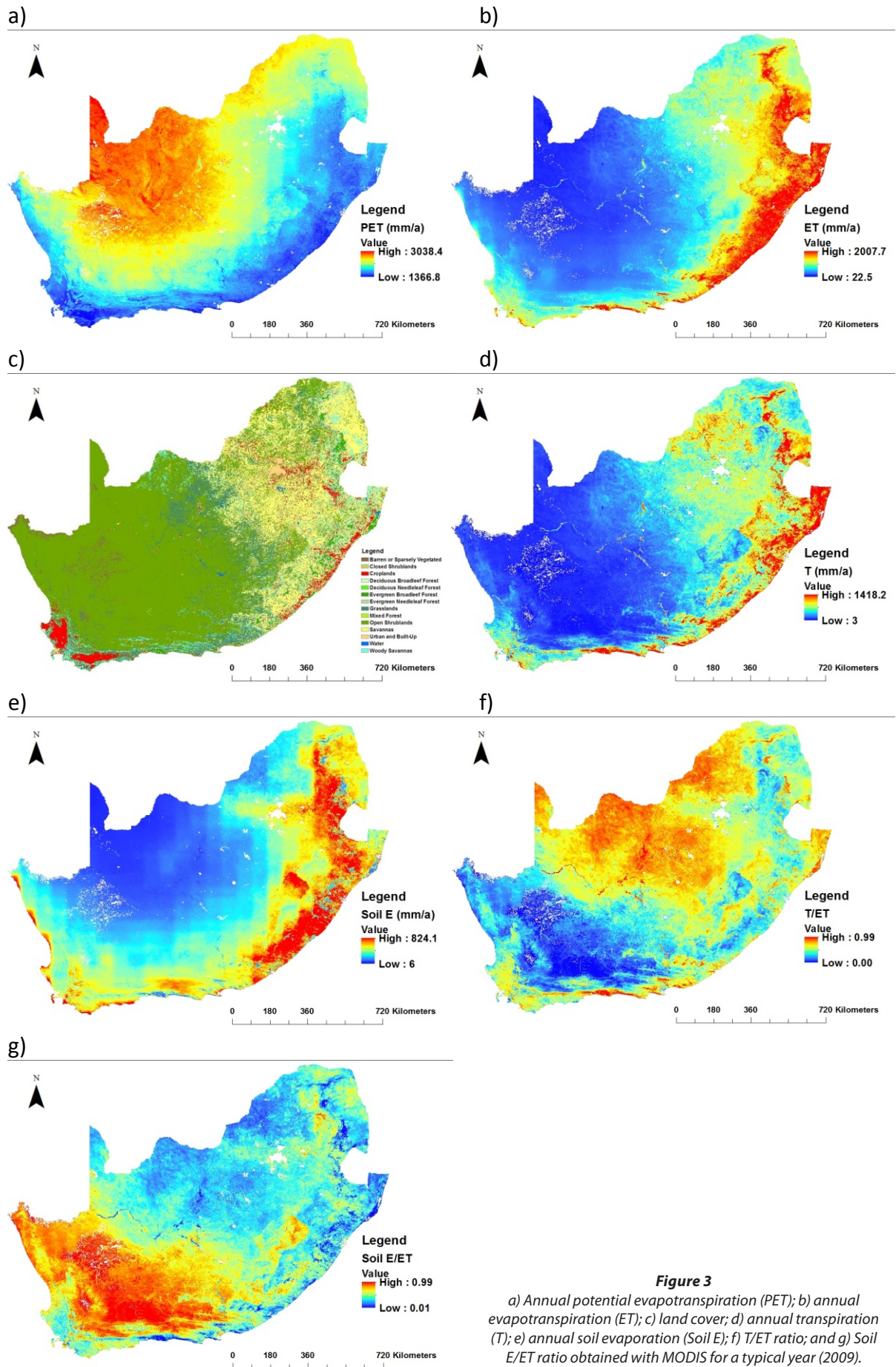
Figure 3

a) Annual potential evapotranspiration (PET); b) annual evapotranspiration (ET); c) land cover; d) annual transpiration (T); e) annual soil evaporation (Soil E); f) T/ET ratio; and g) Soil E/ET ratio obtained with MODIS for a typical year (2009).

TABLE 6
Spearman correlation coefficients of annual potential evapotranspiration (*PET*), actual evapotranspiration (*ET*), canopy and soil evaporation (*E*) and transpiration (*T*) estimated with MODIS products for the period 2000–2012 for South Africa

Variable	PET	ET	Canopy E	Soil E	T	ET/PET	Canopy E/ET	Soil E/ET	T/ET
PET	1	**7.5E-04**	**1.1E-03**	**8.1E-04**	**0.02**	**5.7E-04**	**1.9E-03**	**0.02**	**4.8E-03**
ET	−0.97	1	**1.2E-03**	**8.7E-04**	**0.01**	**6.6E-04**	**2.2E-03**	**0.04**	**0.01**
Canopy E	−0.94	0.93	1	**8.1E-04**	0.06	**1.3E-03**	**6.1E-04**	**0.01**	**1.6E-03**
Soil E	−0.97	0.96	0.97	1	**0.04**	**7.5E-04**	**1.2E-03**	**0.01**	**2.2E-03**
T	−0.7	0.74	0.54	0.59	1	**0.01**	0.12	0.98	0.46
ET/PET	−0.99	0.98	0.93	0.97	0.7	1	**2.3E-03**	**0.02**	**0.01**
Canopy E/ET	−0.9	0.88	0.99	0.93	0.45	0.88	1	**0.01**	**1.3E-03**
Soil E/ET	−0.65	0.6	0.76	0.77	−0.01	0.65	0.77	1	**1.4E-03**
T/ET	0.81	−0.76	−0.91	−0.88	−0.21	−0.8	−0.93	−0.92	1

TABLE 7
Average, median, standard deviation, coefficient of variation, skewness and kurtosis of spatial MODIS variables obtained for South Africa for a typical year (2009); *n*= 1 591 184

Statistical parameter	ET	PET	Soil E	Dry soil E	Wet soil E	T	Tavg	Tday	VPD
Average	307	2 236	122	92	29	156	20.21	22.31	1.97
Median	238	2 251	109	89	20	120	20.00	22.20	1.94
Standard deviation	238	303	77	49	31	151	2.97	2.94	0.82
Coefficient of variation	0.78	0.14	0.63	0.53	1.07	0.97	0.15	0.13	0.42
Skewness	1.33	−0.01	0.85	0.48	1.61	2.27	0.16	0.04	0.12
Kurtosis	2.00	−1.05	0.57	−0.15	2.64	8.46	−1.20	−1.16	−0.95

values lower than averages and the positive skewness indicated that the frequency of observations is biased towards the low value range. For climatic variables (*PET*, *Tavg*, *Tday* and *VPD*), the frequency distribution tended to be symmetrical. Kurtosis is an indication of the shape (peak) of the distribution and varied from a negative number for the climatic variables (frequency distribution function with a shape of an inverted bell with no extreme tail values) to 8.64 for *T* (frequency distribution function with a sharp peak).

Annual values of *PET*, *ET* and its components are strongly dependent on climate (Tables 2 to 5). The highest *PET* values occurred in the semi-arid and arid areas (2 457 mm·a⁻¹ on average) and the lowest under tropical wet conditions (1 892 mm·a⁻¹) (Fig. 3a, Tables 3 and 5). This is consistent with isoreference evaporation maps produced by Savva and Frenken (2002) using ground-based meteorological measurements, and the historic pan evaporation data processed by Watkins (1993). Concerning *ET* and its components, an inverse spatial trend was observed. The highest *ET*, *Canopy E*, *Soil E* and *T* were under tropical conditions and the lowest in arid and semi-arid climate. *ET* was higher in summer rainfall areas compared to winter rainfall areas in some years, and lower in others, depending on rainfall pattern and distribution. *Canopy E* and *Soil E* were generally higher and *T* was lower in winter rainfall areas compared to summer rainfall. This was due to the low-intensity rainfall typically occurring in winter areas (frontal rain brought by cold fronts from the ocean) compared to tropical thunderstorms of high intensity occurring in summer rainfall areas. *Canopy E* in winter rainfall areas (8% of *ET* on average, Table 4) was consistent with the measurement of 6% made by Jovanovic et al. (2013) on fynbos vegetation endemic to this area. *Canopy E* in arid and semi-arid areas was basically negligible due to low rainfall and sparse vegetation. The highest *ET/PET* and *Canopy E/ET*

ratios were in tropical areas (0.38 and 0.18 on average) and the lowest in arid areas (0.05 and 0). The highest *Soil E/ET* ratio was in arid areas due to sparse vegetation (0.52), followed by winter rainfall areas (0.46) due to low intensity rainfall. The highest *T/ET* ratio was in summer rainfall areas (0.63) with high intensity rainfall coinciding with periods of high atmospheric evaporative demand.

In comparative terms, Ahmad et al. (2005) estimated *ET* to be 3.51 mm·d⁻¹ on average for the dominant land class (forest and woodlands) in the Olifants catchment (summer rainfall area), using a LandSat image and SEBAL on 7 January 2002. Meijninger and Jarmain (2014) estimated *ET* of dominant vegetation using MODIS and SEBAL. Annual *ET* was estimated to be 575 mm for native thicket, 520 mm for endemic fynbos and >800 mm for alien invasive and exotic forest plantation species in the Western Cape Province (southwest coastal zone of the winter rainfall region). In the KwaZuluNatal Province (east coast tropical wet region), annual *ET* was estimated to be 875 mm for alien invasive species, 755 for native thicket, 685 mm for savanna and 640 mm for grasslands. The dominant farming taking place along the east coast is with sugarcane. Olivier and Singels (2012), using lysimeters, measured a seasonal *ET* of irrigated sugarcane of between 1 061 and 1 378 mm depending on crop management. These literature data were collected for specific purposes, over different areas and targeted to specific types of vegetation, so a direct comparison with MOD16 ET is difficult. However, the values reported in the literature give a coarse indication that the ranges of *ET* were comparable to those estimated with MOD16 ET.

Data for *ET* and related components were correlated to test the interdependency of key variables in the algorithm. Table 8 summarises *r* obtained for *ET* and related variables per year. For convenience, |*r*| values >0.7 were marked in bold in

TABLE 8
Pearson correlation coefficients (*r*) between yearly evapotranspiration (*ET*) (rows)
and variables used in the MOD16 ET algorithm (columns) (*p*<0.01)

Year	ET vs PET	ET vs Soil E	ET vs Dry Soil E	ET vs Wet Soil E	ET vs T	ET vs Tavg	ET vs Tday	ET vs VPD
2000	−0.73	0.67	0.56	0.76	0.91	−0.43	−0.53	−0.77
2001	−0.71	0.56	0.41	0.71	0.92	−0.43	−0.60	−0.82
2002	−0.72	0.56	0.45	0.68	0.94	−0.58	−0.65	−0.79
2003	−0.74	0.60	0.52	0.67	0.93	−0.42	−0.48	−0.74
2004	−0.76	0.61	0.53	0.69	0.94	−0.48	−0.56	−0.76
2005	−0.75	0.66	0.57	0.73	0.91	−0.60	−0.68	−0.80
2006	−0.73	0.63	0.50	0.74	0.91	−0.38	−0.47	−0.77
2007	−0.73	0.62	0.53	0.72	0.92	−0.58	−0.65	−0.80
2008	−0.73	0.65	0.56	0.73	0.89	−0.56	−0.65	−0.80
2009	−0.72	0.65	0.55	0.72	0.91	−0.45	−0.54	−0.77
2010	−0.73	0.64	0.56	0.72	0.90	−0.46	−0.54	−0.74
2011	−0.68	0.59	0.49	0.70	0.91	−0.44	−0.53	−0.79
2012	−0.72	0.60	0.50	0.71	0.91	−0.53	−0.58	−0.78

Table 8. This value was chosen arbitrarily to represent moderate to high correlation between variables. Attempts to fit non-linear regression functions were made; however this did not result in substantial increases of R^2. Significance tests resulted in probability values tending to 0 in all cases due to the large datasets and degrees of freedom (population number >100 000). The effects of large sample sizes on the *p*-value were discussed by Lin et al. (2003), who suggested procedures and guidelines to overcome this problem.

It is evident from Table 8 that *ET* was driven by atmospheric evaporative demand (*PET*) and strongly correlated to *T* and *VPD*. Analysis by climatic regions indicated that this was particularly true for winter rainfall and arid areas. Daytime average temperature (*Tday*) had higher *r* compared to *Tavg* (exception was tropical wet climate). The correlations between *ET* and *Soil E* were generally poor, with the exception of some years in arid areas. Concerning the directions of the relations, *r* was positive in the relations of *ET* to *Soil E* and *T*; an exception was the tropical wet climate where *ET* was negatively and weakly correlated to *Soil E*, possibly due to the effects of dense vegetation and canopy cover under humid conditions. The correlations between *ET* and climatic variables (*PET*, *Tavg*, *Tday* and *VPD*) had variable strength and were negative, with the exception of the tropical wet climate, where higher temperatures resulted in higher *ET* in most years.

Examples of correlations between key algorithm variables are shown in Fig. 4 for two distinct climatic regions (tropical wet and arid to semi-arid) for a typical year (2009). Evapotranspiration (*ET*) is weakly driven by *PET*, particularly under tropical wet conditions. The negative slope of the linear regression indicates that *ET* is higher when the atmospheric evaporative demand is lower (Figs 4a and b). The correlation coefficient between *ET* and *VPD* was moderate in arid regions (Fig. 4c) and weak in the tropical climate (Fig. 4d). However, the direction of change was the same: higher *VPD* corresponded to lower *ET* (Tanner and Sinclair, 1983). The *VPD* derived from the global coarse-resolution (0.5°x0.66°) MERRA meteorological data cannot always reflect small-scale (1 km) *VPD* variations. As a result, small areas of wetland, springs or irrigated cropland may cause spikes in *ET* at high *VPD* values especially in the arid and semi-arid region. For example, this is visible in Fig. 4c at *VPD* ~ 3.25 kPa. Although outliers

are visible in Figs 4c and d, the bulk of the data points are in the lower part of the graphs. Similar relations were generally observed for *ET* in relation to daily average and daytime temperature (data not shown). Figures 4e to h show the relations between *ET* and its components *Soil E* and *T*. The data distribution of *ET* vs. *Soil E* has a fanshape: it is controlled by *T* in the lower range of *Soil E*, whilst *Soil E* is usually the limiting factor in the high range of its values. The moderate R^2 in the arid climate (Fig. 4e) indicates that *Soil E* is an important component of *ET* where vegetation is sparse and canopy cover is low. This is not the case in the tropical climate (Fig. 4f), where a low R^2 was observed with a negative slope of the linear regression, indicating that, in predominantly dense vegetation, *T* is the main controlling factor. Similar directions and relations were observed between *ET* and the separate components of *Dry Soil E* and *Wet Soil E* (data not shown). Amongst all factors analysed, *ET* had the strongest dependence on *T* (Figs 4g and h). The fanshape of the data plot is visible for arid areas (Fig. 4g), where the *ET* is controlled by *Soil E* in the lower range of *T*. In areas with dense vegetation, the R^2 of the linear regression between *ET* and *T* was high and the fanshape of the data plot almost straightened completely (Fig. 4h). The *T* portion of the algorithm appears to be suitable for humid regions where *ET* is limited by available energy and stomatal resistance is regulated by air temperature and *VPD*. However, in dry regions, additional controlling factors like soil water supply play a role in the estimation of *ET* (Mu et al., 2007b).

CONCLUSIONS

Satellite Earth observations will be of huge importance in a variety of applications in future. Remote sensing–based methods have scope in routine applications for water and land resource planning and management, as well as in scientific research on physical, biogeochemical and ecological processes. In this study, we presented a first evaluation of MOD16 ET and related products for South Africa.

Average *ET* in South Africa (2000–2012) was estimated to be 303 mm·a^{-1} or 371.6 x 10^9 mm·a^{-1} (14% of *PET* and 67% of rainfall), mainly in the form of plant transpiration (53%) and *Soil E* (39%). Direct evaporation from the vegetation canopy was a minor component of *ET* (9% on average).
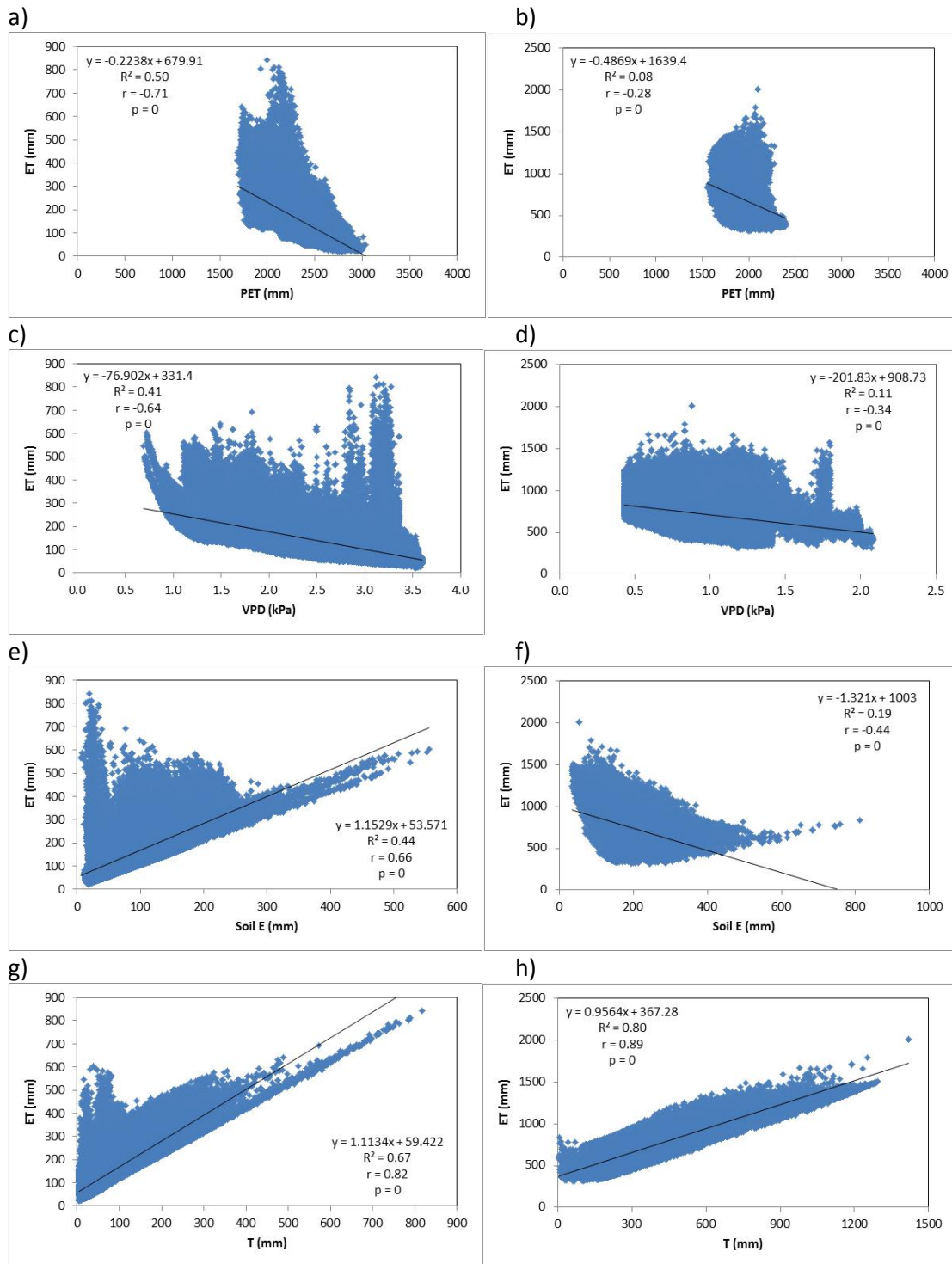
Figure 4
*Linear regressions of MODIS evapotranspiration (ET) vs. potential evapotranspiration (PET), vapour
pressure deficit (VPD), soil evaporation (Soil E) and transpiration (T) for arid and semi-arid region
(a, c, e, g) and tropical wet climate (b, d, f, h) for a typical year (2009).*

Evapotranspiration showed a slight tendency to decrease over the period 2000–2012 in all climatic regions except in the south of the country (winter rainfall areas), although annual variations in *ET* resulted in the 13-year trends not being statistically significant. Rainfall and atmospheric evaporative demand are the main climatic variables driving *ET* and particularly its

transpiration component. The highest *PET* values occurred in the semi-arid and arid areas (2 457 mm·a^{-1} on average) and the lowest under tropical wet conditions (1 892 mm·a^{-1}). Inversely, the highest *ET*, *Canopy E*, *Soil E* and *T* were under tropical conditions and the lowest in arid and semi-arid climate. Vapour pressure deficit (*VPD*) is an important climatic variable in arid

and winter rainfall areas. The relation of *ET* to daytime average temperature generally had a higher correlation coefficient compared to *Tavg* in all climatic areas, except under tropical conditions. Evapotranspiration (*ET*) is strongly dependent on *T* in all climatic regions, and occasionally on *Soil E* in dry areas with sparse vegetation.

The MOD16 ET algorithm can be suitable to identify temporal changes and for relative comparisons of data between climatic regions. In absolute terms, MOD16 ET underestimated *ET* by 15% for water balance closure at national scale. These results, however, open up the opportunity to improve and test the algorithm for *ET* estimation, by accounting for both atmospheric demand limiting and soil water supply limiting conditions in the next research phase. The relatively coarse resolution of ~1 km² pixels may have implications for applications in restricted areas, especially in heterogeneous vegetation, land use/cover and landscape.

ACKNOWLEDGMENTS

REFERENCES

AHMAD M, MAGAGULA TF, LOVE D, KONGO V, MUL ML and KINOTI J (2005) Estimating actual evapotranspiration through remote sensing techniques to improve agricultural water management: A case study in the transboundary Olifants catchment in the Limpopo Basin, South Africa. In: *Proceedings of the 6th WaterNet/WARFSA/GWP Annual Symposium*, 1–4 November 2005, Ezulwini, Swaziland.

ALLEN RG, PEREIRA LS, RAES D and SMITH M (1998) *Crop Evapotranspiration: Guidelines for Computing Crop Water Requirements*. Irrigation and Drainage Paper 56. United Nations Food and Agriculture Organization, Rome. 300 pp.

ALLEN RG, TASUMI M and TREZZA R (2007a) Satellite-based energy balance for mapping evapotranspiration with internalized calibration (METRIC) – Model. *J. Irrig. Drain. Eng.* **133** (4) 380–394.

ALLEN RG, TASUMI M, MORSE A, TREZZA R, WRIGHT JL, BASTIAANSSEN W, KRAMBER W, LORITE I and ROBINSON CW (2007b) Satellite-based energy balance for mapping evapotranspiration with internalized calibration (METRIC) – Applications. *J. Irrig. Drain. Eng.* **133** (4) 395–406.

BALDOCCHI D, FALGE E, GU G, OLSON R, HOLLINGER D, RUNNING S, ANTHONI P, BERNHOFER Ch, DAVIS K, EVANS R and co-authors (2001) FLUXNET: A new tool to study the temporal and spatial variability of ecosystem-scale carbon dioxide, water vapor, and energy flux densities. *Bull. Amer. Meteor. Soc.* **82** 2415–2434.

BASTIAANSSEN WGM, MENENTI M, FEDDES RA and HOLTSLAG AAM (1998a) A remote sensing Surface Energy Balance Algorithm for Land (SEBAL) 1. Formulation. *J. Hydrol.* **212–213** 198–212.

BASTIAANSSEN WGM, PELGRUM H, WANG J, MA Y, MORENO JF, ROERINK GJ and VAN DER WAL T (1998b) A remote sensing Surface Energy Balance Algorithm for Land (SEBAL) 2. Validation. *J. Hydrol.* **212–213** 213–229.

BUGAN RDH, JOVANOVIC N and DE CLERCQ WP (2012) The water balance of a seasonal stream in the semi-arid Western Cape (South Africa). *Water SA* **38** (2) 201–212.

CLEUGH HA, LEUNING R, MU Q and RUNNING SW (2007) Regional evaporation estimates from flux tower and MODIS satellite data. *Remote Sens. Environ.* **106** 285–304.

DI RIENZO JA, CASANOVES F, BALZARINI MG, GONZALEZ L, TABLADA M and ROBLEDO CW (2012) Grupo InfoStat, FCA, Universidad Nacional de Córdoba, Argentina. URL: http://www.infostat.com.ar (Accessed 23 October 2014).

DWAF (DEPARTMENT OF WATER AFFAIRS AND FORESTRY, SOUTH AFRICA) (2004) *National Water Resource Strategy. 1st Edition*. Chapter 2. Department of Water Affairs and Forestry, Pretoria. 54 pp.

DWAF (DEPARTMENT OF WATER AFFAIRS AND FORESTRY, SOUTH AFRICA) (2005) Groundwater Resource Assessment II – Task 3aE Recharge. Department of Water Affairs and Forestry, Pretoria. 129 pp.

FISHER JB, TU K and BALDOCCHI DD (2008) Global estimates of the land atmosphere water flux based on monthly AVHRR and ISLSCPII data, validated at FLUXNET sites. *Remote Sens. Environ.* **112** (3) 901–19.

FRENKEN K (2005) *Irrigation in Africa in Figures – Aquastat Survey 2005*. United Nations Food and Agriculture Organization, Rome. 53 pp.

JI L and GALLO K (2006) An agreement coefficient for image comparison. *Photogram. Eng. Remote Sens.* **72** (7) 823–833.

JIMENEZ C, PRIGENT C, MUELLER B, SENEVIRATNE SI, McCABE MF, WOOD EF, ROSSOW WB, BALSAMO G, BETTS AK, DIRMEYER PA and co-authors (2011) Global intercomparison of 12 land surface heat flux estimates. *J. Geophys. Res.* **116** (D02102) 1–27.

JOVANOVIC N and ISRAEL S (2012) Critical review of methods for the estimation of actual evapotranspiration in hydrological models. In: Irmak A (ed.) *Evapotranspiration – Remote Sensing and Modelling*. Intech, Rijeka, Croatia.

JOVANOVIC N, BUGAN R and ISRAEL S (2013) Quantifying the evapotranspiration component of the water balance of Atlantis Sand Plain Fynbos (South Africa). In: Stavros A and Stricevic R (eds.) *Evapotranspiration – An Overview*. Intech, Rijeka, Croatia.

JUSTICE CO, TOWNSHEND JRG, VERMOTE EF, MASUOKA E, WOLFE RE, SALEOUS N, ROY DP and MORISETTE JT (2002) An overview of MODIS land data processing and product status. *Remote Sens. Environ.* **83** 3–15.

KORZOUN VI, SOKOLOV AA, BUDYKO MI, VOSKRESENSKY KP and KALININ GP (1978) *World Water Balance and Water Resources of the Earth (English)*. Studies and Reports in Hydrology (UNESCO), no. 25/United Nations Educational, Scientific and Cultural Organization, 75 Paris (France); International Hydrological Decade. USSR National Committee, Moscow, USSR. 663 pp.

L'VOVICH MI and WHITE GF (1990) Use and transformation of terrestrial water systems. In: Turner BL, Clark WC, Kates RW, Richards JF, Mathews JT and Meyer WB (eds.) *The Earth as Transformed by Human Action*. Cambridge University Press, Cambridge, UK.

LIN M, LUCAS HC Jr and SHMUELI G (2003) Too big to fail: Large samples and the pvalue problem. *Inf. Syst. Res.* **24** (4) 906–917.

LYNCH SD and SCHULZE RE (2006) South African atlas of climatology and agrohydrology – Rainfall database. WRC Report No. 1489/1/06, Section 2.2. Water Research Commission, Pretoria.

MEIJNINGER WML and JARMAIN C (2014) Satellite based annual evaporation estimates of invasive alien plant species in South Africa. *Water SA* **40** (1) 95–107.

MONTEITH JL (1965) Evaporation and environment. *Symp. Soc. Exp. Biol.* **19** 205–234.

MU Q, HEINSCH FS, ZHAO M and RUNNING SW (2007a) Development of a global evapotranspiration algorithm based on MODIS and global meteorology data. *Remote Sens. Environ.* **111** 519–536.

MU Q, ZHAO M, HEINSCH FS, LIU M, TIAN H and RUNNING SW (2007b) Evaluating water stress controls on primary production in biogeochemical and remote sensing based models. *J. Geophys. Res.* **112** (G01012) 1–13.

MU Q, ZHAO M and RUNNING SW (2011) Improvements to a MODIS global terrestrial evapotranspiration algorithm. *Remote Sens. Environ.* **115** 1781–1800.

MUELLER B, SENEVIRATNE SI, JIMENEZ C, CORTI T, HIRSCHI M, BALSAMO G, CIAIS P, DIRMEYER P, FISHER JB, GUO Z and co-authors (2011) Evaluation of global observations-based evapotranspiration datasets and IPCC AR4 simulations. *Geophys. Res. Lett.* **38** (L06402) 1–7.

MYNENI RB, HOFFMAN S, KNYAZIKHIN Y, PRIVETTE JL, GLASSY J, TIAN T, WANG Y, SONG X, ZHANG Y, SMITH GR and co-authors (2002) Global products of vegetation leaf area and fraction absorbed PAR from year one of MODIS data. *Remote Sens. Environ.* **83** (1–2) 214–231.

OLIVIER FC and SINGELS A (2012) The effect of crop residue layers on evapotranspiration, growth and yield of irrigated sugarcane. *Water SA* **38** (1) 77–86.

PRIESTLEY CHB and TAYLOR RJ (1972) On the assessment of surface heat flux and evaporation using large scale parameters. *Mon. Weather Rev.* **100** 81–92.

SAVVA AP and FRENKEN K (2002) Crop Water Requirements and Irrigation Scheduling. Irrigation Manual. Module 4 FAO Sub-Regional Office for East and Southern Africa. Fontline Electronic Publishing, Harare, Zimbabwe. 122 pp.

SU Z (2002) The Surface Energy Balance System (SEBS) for estimation of turbulent heat fluxes. *Hydrol. Earth Syst. Sci.* **6** 85–99.

TANNER CB and SINCLAIR TR (1983) Efficient water use in crop production: research or re-search? In: Taylor HM, Jordan WR, Sinclair TR (eds.) *Limitations to Efficient Water Use in Crop Production.* American Society of Agronomy, Madison, WI, USA.

VEGTER JR (1995) An explanation of a set of national groundwater maps. WRC Report No. TT 74/95. Water Research Commission, Pretoria.

WATKINS DA (1993) The relationship between daily and monthly pan evaporation and rainfall totals in Southern Africa. MSc thesis, Rhodes University.

ZHAO M, HEINSCH FA, NEMANI R and RUNNING SW (2005) Improvements of the MODIS terrestrial gross and net primary production global data set. *Remote Sens. Environ.* **95** 164–176.

ERRATUM

Erratum for *Water SA* 41 (1) 79–90, originally published in January 2015:

Page 79, line 4 of abstract:
'481.4 x 10^9 $m^3 \cdot a^{-1}$' should be replaced with '371.6 x 10^9 $m^3 \cdot a^{-1}$'.

Page 83, left column, last paragraph should read (please note the change in units):
'In absolute terms, MOD16 ET estimated an average water loss to the atmosphere of 371.6 x 10^9 $m^3 \cdot a^{-1}$ for the country (Table 1). Assuming an average rainfall of 450 $mm \cdot a^{-1}$, corresponding to 553 x 10^9 $m^3 \cdot a^{-1}$, it was calculated that 67% of rainfall water evaporates. It was estimated that runoff is about 50 x 10^9 $m^3 \cdot a^{-1}$ or 9% of rainfall (DWAF, 2004) and that groundwater recharge is about 30 x 10^9 $m^3 \cdot a^{-1}$ or 5% of rainfall (Vegter, 1995; DWAF, 2005). Frenken (2005) estimated water withdrawal in South Africa to be 12.5 x 10^9 $m^3 \cdot a^{-1}$ in 2000.'

Page 87, right column, last paragraph (please note the change in units):
'371.6 x 10^9 $mm \cdot a^{-1}$' should be replaced with '371.6 x 10^9 $m^3 \cdot a^{-1}$'.